Supporting Information

H/OH substitution constructing K–O coordinated bond and introducing homochirality for the design of a 3D hybrid double perovskite multiferroic

Mei-Ling Ren,[a] Ze-Jiang Xu,[a] Hua-Kai Li,[a] Zi-Ao Qiu,[a] Liang-Han Shen,[a] Xiang Zhang,[a] Chao Shi,[a] Na Wang,*[a] Heng-Yun Ye,*[a] and Le-Ping Miao*[a]

[a] Chaotic Matter Science Research Center, Department of Materials, Metallurgy and Chemistry, Jiangxi University of Science and Technology, Ganzhou 341000, P.R. China

*Correspondence and requests for materials should be addressed to L.P.M. (miaoleping@jxust.edu.cn).

Supplementary Index

Experimental

Sample preparation

General Measurements

X-ray diffraction experiments

Supplemental Fig.s

Fig. S1. PXRD patterns of compound R3PBKC (a) ,3PBKC (b), PBC (c) and 3MPBKC (d) at 298 K.

Fig. S2. Thermogravimetric analysis (TGA) curve of R3PBKC around 300–1100 K.

Fig. S3. Packing diagrams of PBC in 300 K (a) and 3MPBKC in 268 K (b).

Fig. S4. Packing diagrams of R3PBKC in LTP(a), ITP1 (b), ITP2 (c), and HTP (d).

Fig. S5. The packing model of molecular structures of P3BKC in ITP_1 along the *a*-axis (a) and *b*-axis (b).

Fig. S6. Bond angle of R3PBKC at ITP_1 (a), ITP_2 (b), and HTP (c).

Fig. S7. Temperature dependence of the real dielectric constant of R3PBKC along the (a) *a*, (b) *b*, and (c) *c* axis during cooling.

Fig. S8. The imaginary part dielectric constant (ε'') of the powder sample of R3PBKC is measured at different heating frequencies.

Fig. S9. DSC curves of PBC at 210–245 K (a), 3PBKC at 330–370 K (b) and 3MPBKC at 330–370 K (c).

Fig. S10. Temperature dependence of the real dielectric constant of PBC (a) and 3PBKC (b) during cooling.

Fig. S11. The *P–E* hysteresis loops of R3PBKC in the *a*-axis and *b*-axis at 333 K.

Fig. S12. Temperature-dependence of the SHG intensity for 3PBKC in a heating–cooling cycle (a). The *P–E* hysteresis loops of 3PBKC in the *a*-axis at 308 K (b).

Fig. S13. Ultraviolet−visible (UV−vis) absorption spectrum of R3PBKC. Inset: Tauc plot with an estimated band gap of 3.18 eV.

Supplemental Tables

Table S1. Crystal Data and Structure Refinement Details for 3PBKC, PBC and 3MPBKC at 273 K, 300 K, and 268 K, respectively.

Table S2. Crystal Data and Structure Refinement Details for R3PBKC at 302 K and 353 K.

Table S3. Crystal Data and Structure Refinement Details for R3PBKC at 386 K and 413 K.

Table S4. Selected bond lengths [Å] and angles [°] for R3PBKC at 302 K.

Table S5. Selected bond lengths [Å] and angles [°] for R3PBKC at 353 K.

Table S6. Selected bond lengths [Å] and angles [°] for R3PBKC at 386 K.**Table S7.** Selected bond lengths [Å] and angles [°] for R3PBKC at 413 K.

Experimental

Sample preparation.

Materials: (*R*)-hydroxypyrrolidine (≥99%, Shanghai Haohong Bio-pharmaceutical Technology Co., Ltd.). 3-pyrrolidinol (97%, Shanghai Haohong Bio-pharmaceutical Technology Co., Ltd.). Pyrrolidine (99%, ShangHai Tian Scientific Co., Ltd.). 3-methylpyrrolidine (99%, ShangHai Tian Scientific Co., Ltd.). KCl (≥99.5%, Shanghai Tian Scientific Co., Ltd.). $BiCl_3$ (Shanghai Macklin Biochemical Co., Ltd.). HCl (36% ~ 38%, Jiangxi Xinguang Electronic Technology Co., Ltd.). All chemicals are commercially available and used directly without purification.

Synthesis of compound R3PBKC: (*R*)-hydroxypyrrolidine, KCl and $BiCl_3$ were weighed at stoichiometry 2:1:1, respectively. Using HCl (36% ~ 38%) solution as the solvent, it is slowly evaporated on a 303 K constant temperature heating table. After about seven days, a mixture containing precipitated crystals and mother liquor is obtained.

Synthesis of compound 3PBKC: 3-pyrrolidinol, KCl and $BiCl_3$ were weighed at stoichiometry 2:1:1, respectively. Using HCl (36% ~ 38%) solution as the solvent, it is slowly evaporated on a 303 K constant temperature heating table. After about seven days, a mixture containing precipitated crystals and mother liquor is obtained.

Synthesis of compound PBC: Pyrrolidine and $BiCl_3$ were weighed at stoichiometry 3:1, respectively. Using HCl (36% ~ 38%) solution as the solvent, it is slowly evaporated on a 318 K constant temperature heating table. After about ten days, a mixture containing precipitated crystals and mother liquor is obtained.

Synthesis of compound 3MPBKC: 3-methylpyrrolidine, KCl and $BiCl_3$ were weighed at stoichiometry 2:1:1, respectively. Using HCl (36% ~ 38%) solution as the solvent, it is slowly evaporated on a 318 K constant temperature heating table. After about seven days, a mixture containing precipitated crystals and mother liquor is obtained.

General Measurements.

The Powder X-ray Diffraction (PXRD) was measured at a measurement angle of 5°–50° and a scan rate of 5°/min on the Rigaku D/MAX 2000 PC X-ray diffractometer. And the X-ray wavelength is 0.15406 nm. Differential scanning calorimetry (DSC) was

measured on a DSC 214 Polyma instrument under a nitrogen atmosphere with a heating/cooling rate of 10 K/min. The dielectric measurements of compound R3PBKC were carried out on a Tonghui TH2828A impedance analyzer: the polycrystals of compound R3PBKC were compacted into tight sheets, and the two sides were coated with silver glue and tested in the temperature range of 300 K to 400 K, 500 Hz, 1 kHz, 5 kHz, 10 kHz, 100 kHz and 1 MHz of composite dielectric constant ($\varepsilon_r = \varepsilon' - i\varepsilon''$) changes with temperature. For second harmonic generation (SHG) measurements, an unexpanded laser beam with low divergence (pulsed Nd:YAG at a wavelength of 1064 nm, 5 ns pulse duration, 1.6 MW peak power, 10 Hz repetition rate) was used. The system is based on the theory of KURTZ about the SHG of crystalline powders. The size of the measured samples is about 200 mesh. The ferroelastic domain observations were detected with an Olympus BX51TRF optical polarizing microscope. The temperature remained stable with an accuracy of 0.2 K by using an INSTEC HCC602 cooling/heating stage. The *P*−*E* hysteresis loops were measured on a Radiant Precision Premier II. The instrument consists of Agilent 33500B (a waveform generator), Trek model 609E−6 (a high−voltage waveform amplifier), and Keithley 6517B (an electrometer).

X-ray diffraction experiments.

Variable-temperature X-ray diffraction analysis was carried out using a Rigaku synergy diffractometer with Mo-Kα radiation (λ = 0.71073 Å). Data collection, cell refinement, and data reduction were performed using CrysAlisPro (version 1.171.41.112a) XtaLAB Synergy-R online system. The structures were solved by the direct method and refined by the full-matrix method based on F^2 using the OLEX2 and SHELXTL (2018) software package. All non-hydrogen atoms were refined anisotropically and the positions of all hydrogen atoms were generated geometrically. The organic cations were not modeled according to the chemical sense, because of the highly disordered form at the high-temperature phase. Detailed crystallographic data are recorded in **Tables S1–S7**. CCDC number: 2412865–2412871 contains supplemental crystallographic data for this article. These data are freely available from the Cambridge Crystallographic Data Centre.

Supplemental Fig.s

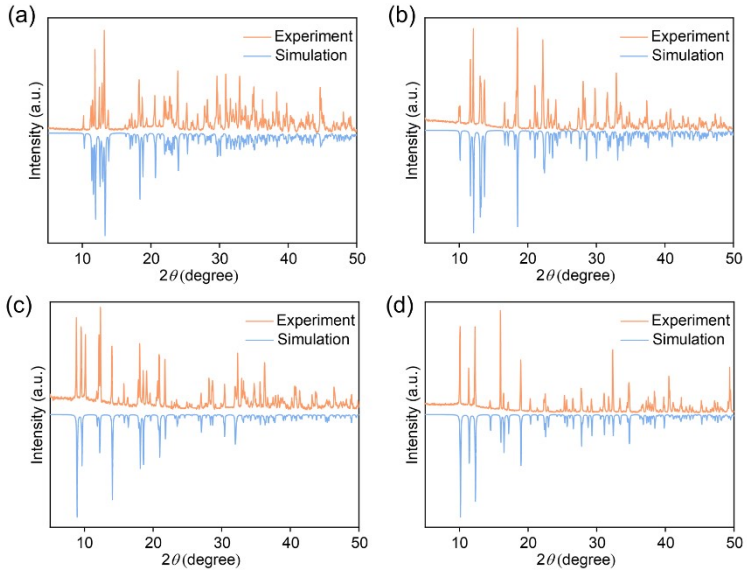

Fig. S1. PXRD patterns of compound R3PBKC (a) ,3PBKC (b), PBC (c) and 3MPBKC (d) at 298 K.

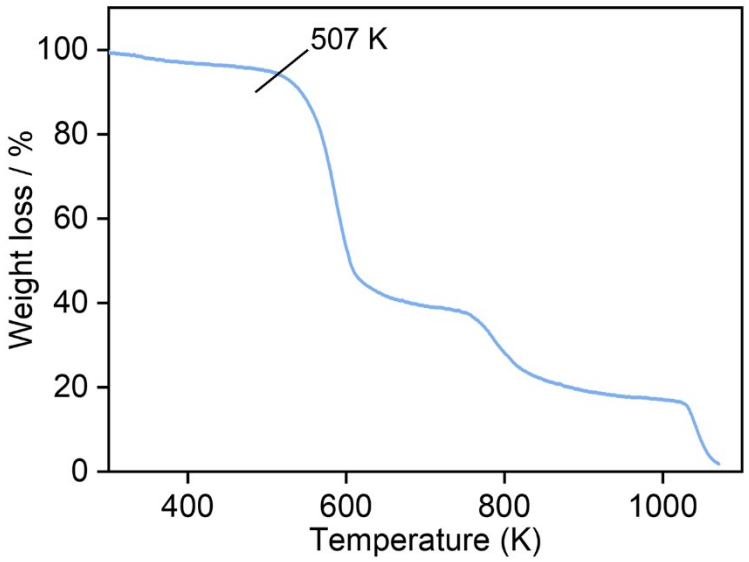

Fig. S2. Thermogravimetric analysis (TGA) curve of R3PBKC around 300–1100 K.

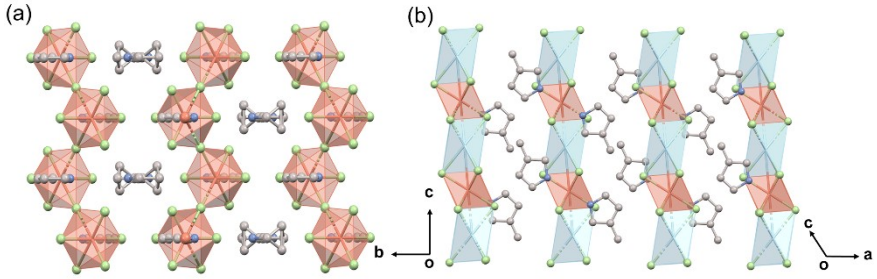

Fig. S3. Packing diagrams of PBC in 300 K (a) and 3MPBKC in 268 K (b).

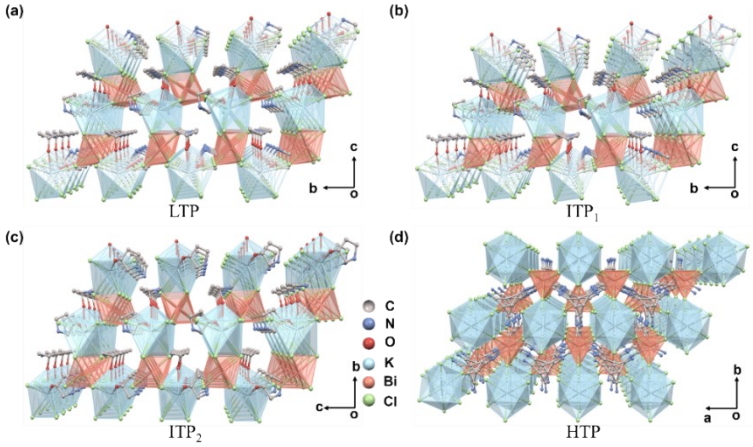

Fig. S4. Packing diagrams of R3PBKC in LTP (a), ITP_1 (b), ITP_2 (c), and HTP (d).

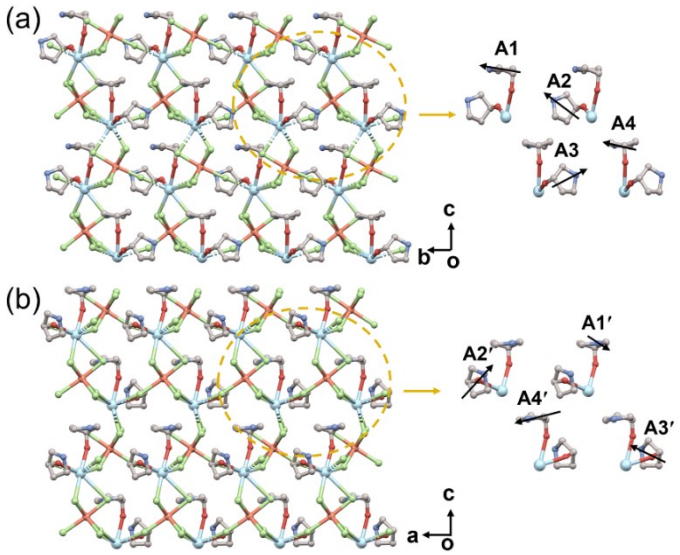

Fig. S5. The packing model of molecular structures of R3PBKC in ITP_1 along the *a*-axis (a) and *b*-axis (b).

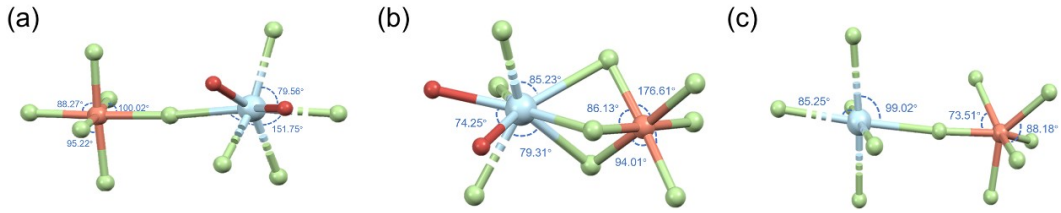

Fig. S6. Bond angle of R3PBKC at ITP_1 (a), ITP_2 (b), and HTP (c).

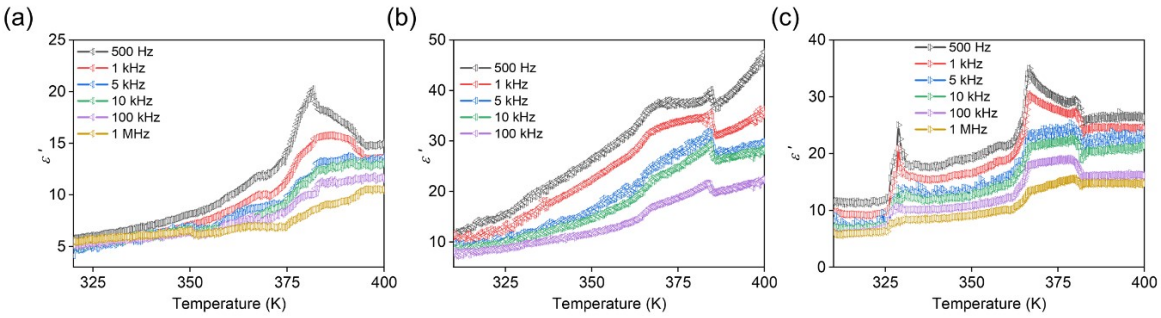

Fig. S7. Temperature dependence of the real dielectric constant of R3PBKC along the (a) *a*, (b) *b*, and (c) *c* axis during cooling.

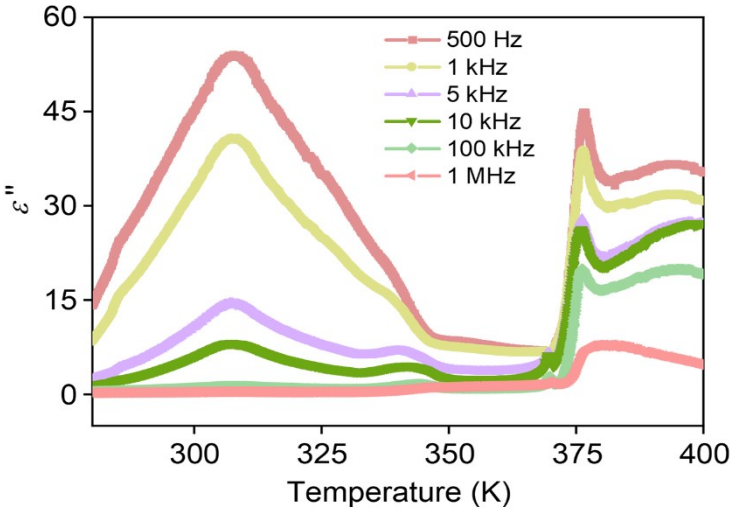

Fig. S8. The imaginary part dielectric constant (ε'') of the powder sample of R3PBKC is measured at different heating frequencies.

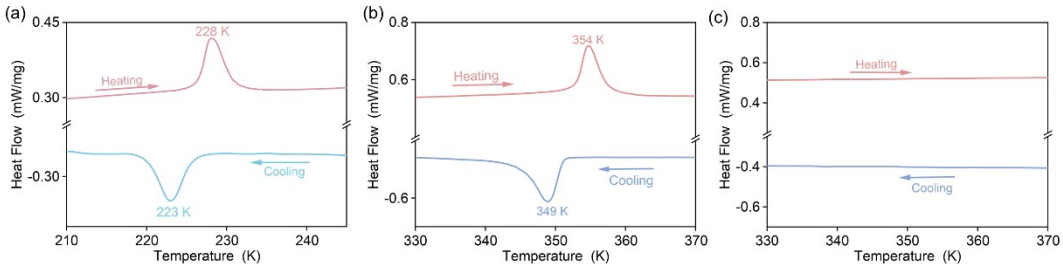

Fig. S9. DSC curves of PBC at 210–245 K (a), 3PBKC at 330–370 K (b) and 3MPBKC at 330–370 K (c).

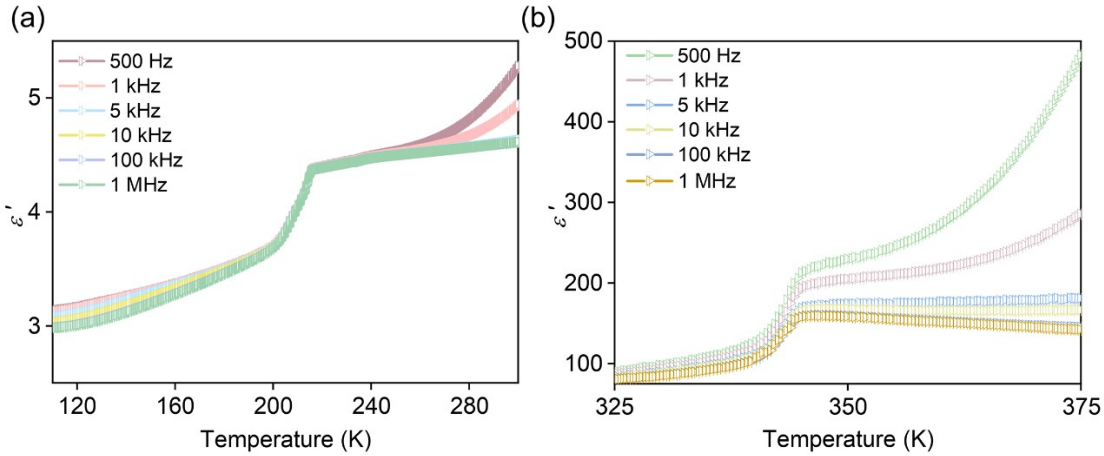

Fig. S10. Temperature dependence of the real dielectric constant of PBC (a) and 3PBKC (b) during cooling.

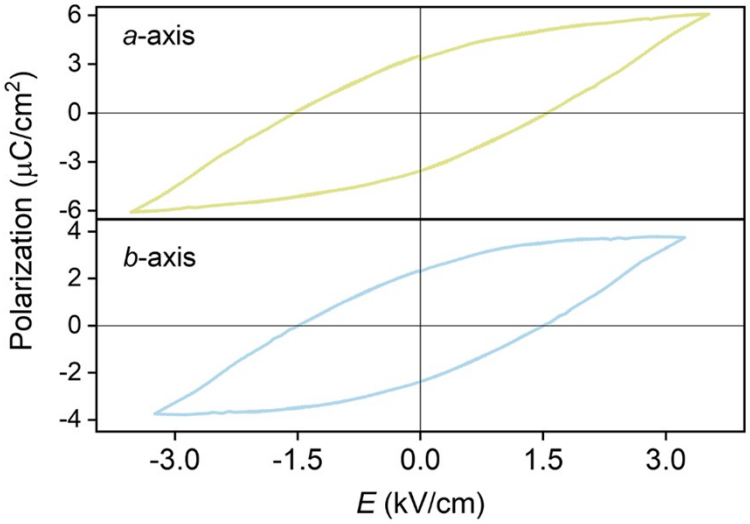

Fig. S11. The *P*–*E* hysteresis loops of R3PBKC in the *a*-axis and *b*-axis at 333 K.

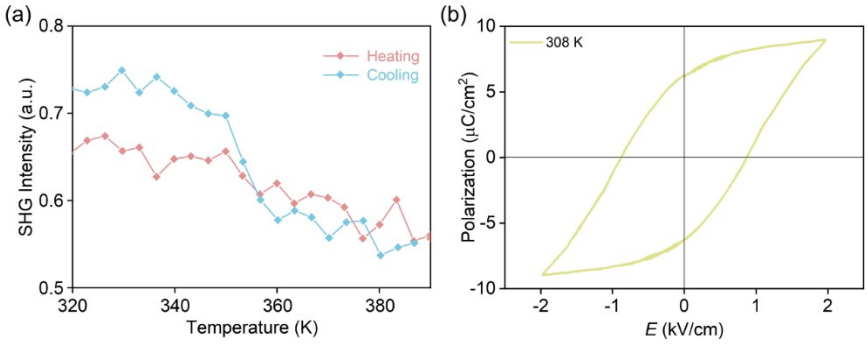

Fig. S12. Temperature-dependence of the SHG intensity for 3PBKC in a heating–cooling cycle (a). The *P*–*E* hysteresis loops of 3PBKC in the *a*-axis at 308 K (b).

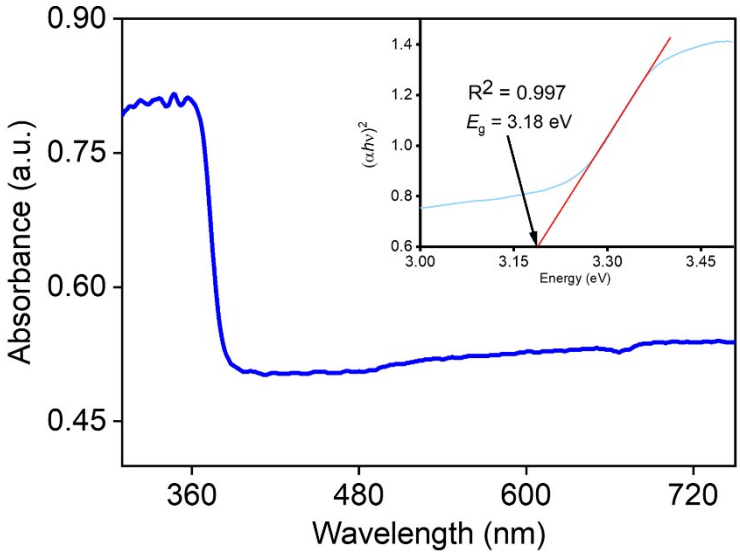

Fig. S13. Ultraviolet−visible (UV−vis) absorption spectrum of R3PBKC. Inset: Tauc plot with an estimated band gap of 3.18 eV.

Supplemental Tables

Table S1. Crystal Data and Structure Refinement Details for 3PBKC, PBC and 3MPBKC at 273 K, 300 K, and 268 K, respectively.

Compunds	3PBKC	PBC	3MPBKC
T / *K*	273 K	300 K	268 K
Formula weight	637.04	903.80	633.09
Empirical formula	$C_8H_{20}BiCl_6KN_2O_2$	$C_9H_{17}BiCl_5N_2$	$C_{10}H_{24}BiCl_6KN_2$
Crystal system	monoclinic	orthorhombic	monoclinic
Space group	*Cc*	*Pnma*	*C*2/*m*
a / Å	8.4070(4)	11.7529(6)	17.5172(12)
b / Å	17.4670(9)	8.1448(4)	7.8780(5)
c / Å	13.4096(6)	18.3261(13)	7.7740(5)
α / °	90	90	90
β / °	93.585(5)	90	95.646(6)
γ / °	90	90	90
V / Å^3	1965.28(17)	1754.27(18)	1067.61(12)
Z	4	4	2
D_{calc} / g·cm^{-3}	2.153	2.050	1.969
μ / mm^{-1}	9.999	10.795	9.196
F(000)	1208.0	1020.0	604.0
2*θ range* / °	4.664−61.82	4.118−61.728	4.674−61.02
Reflns collected	9009	10136	3500
Independent reflns (R_{int})	6198(0.0603)	2939(0.0313)	1741(0.0344)
No. of parameters	185	97	61
R_1[a], wR_2[b] [$I>2\sigma(I)$]	0.0498, 0.1315	0.0550, 0.1530	0.0394, 0.0974
R_1, wR_2 [all data]	0.0546, 0.1344	0.0828, 0.1686	0.0404, 0.0978
GOF	1.070	1.038	1.190
Δ*ρ*[c] / e·Å^{-3}	2.75, −1.68	1.04, −0.99	1.48, −1.64
CCDC	2412865	2412866	2412871

[a] $R_1 = \Sigma||F_o|-|F_c||/|F_o|$; [b] $wR_2 = [\Sigma w(F_o^2-F_c^2)^2]/\Sigma w(F_o^2)^2]^{1/2}$; [c] maximum and minimum residual electron density.

Table S2. Crystal Data and Structure Refinement Details for R3PBKC at 302 K and 353 K.

R3PBKC		
T / *K*	302 K	353 K
Formula weight	1274.08	1272.06
Empirical formula	$C_{16}H_{40}Bi_2Cl_{12}K_2N_4O_4$	$C_{16}H_{38}Bi_2Cl_{12}K_2N_4O_4$
Crystal system	triclinic	triclinic
Space group	*P*1	*P*1
a / Å	8.6103(3)	8.6922(2)
b / Å	9.5297(4)	9.3395(3)
c / Å	13.3411(4)	13.4833(3)
α / °	85.529(3)	86.838(2)
β / °	86.550(2)	87.464(2)
γ / °	64.426(4)	65.957(3)
V / Å^3	984.00(7)	997.81(5)
Z	1	1
D_{calc} / g·cm^{-3}	2.150	2.117
μ / mm^{-1}	9.985	9.847
F(000)	604.0	602.0
2*θ range* / °	4.746−61.916	4.78−61.882
Reflns collected	14015	14441
Independent reflns (R_{int})	12514(0.0439)	7815(0.0338)
No. of parameters	367	364
R_1[a], wR_2[b] [$I>2\sigma(I)$]	0.0366, 0.0767	0.0336, 0.0736
R_1, wR_2 [all data]	0.0457, 0.0794	0.0423, 0.0760
GOF	0.970	0.985
$\Delta\rho$[c] / e·Å^{-3}	1.11, −0.97	1.28, −0.83
CCDC	2412867	2412868

[a] $R_1 = \Sigma||F_o|-|F_c||/|F_o|$; [b] $wR_2 = [\Sigma w(F_o^2-F_c^2)^2]/\Sigma w(F_o^2)^2]^{1/2}$; [c] maximum and minimum residual electron density.

Table S3. Crystal Data and Structure Refinement Details for R3PBKC at 386 K and 413 K.

R3PBKC		
T / *K*	386 K	413 K
Formula weight	616.88	719.04
Empirical formula	$C_8Cl_6BiKN_2O_2$	$C_{12}Cl_6BiKO_6$
Crystal system	monoclinic	hexagonal
Space group	$P2_1$	$P6_322$
a / Å	8.8088(9)	9.3090(15)
b / Å	13.5482(9)	9.3090(15)
c / Å	9.3421(12)	13.5171(12)
α / °	90	90
β / °	115.166(14)	90
γ / °	90	120
V / Å^3	1009.1(2)	1014.4(3)
Z	2	2
D_{calc} / g·cm^{-3}	2.030	2.295
μ / mm^{-1}	9.734	9.710
F(000)	564.0	684.0
2*θ range* / °	4.818−61.612	5.052−50.042
Reflns collected	13553	4266
Independent reflns (R_{int})	5008(0.0532)	610(0.0707)
No. of parameters	181	42
R_1[a], wR_2[b] [$I>2\sigma(I)$]	0.0501, 0.1252	0.1349, 0.3072
R_1, wR_2 [all data]	0.1044, 0.1442	0.1668, 0.3378
GOF	0.918	1.241
$\Delta\rho$[c] / e·Å^{-3}	1.29, −1.15	1.40, −2.12
CCDC	2412869	2412870

[a] $R_1 = \Sigma||F_o|-|F_c||/|F_o|$; [b] $wR_2 = [\Sigma w(F_o^2-F_c^2)^2]/\Sigma w(F_o^2)^2]^{1/2}$; [c] maximum and minimum residual electron density.

Table S4. Selected bond lengths [Å] and angles [°] for R3PBKC at 302 K.

302 K			
Cl10—Bi1—Cl11	89.30 (11)	Cl6—Bi2—Cl5	129.86 (8)
Cl10—Bi1—Cl7	176.84 (12)	Cl5—Bi2—Cl1	50.63 (8)
Cl11—Bi1—Cl7	88.77 (11)	Cl1—Bi2—Cl3	85.05 (11)
Cl10—Bi1—Cl12	87.48 (10)	Cl2—Bi2—Cl3	55.97 (9)
Cl11—Bi1—Cl12	89.07 (10)	Cl8iv—K1—Cl4	86.22 (12)
Cl7—Bi1—Cl12	56.60 (9)	Cl8iv—K1—Cl6	148.35 (14)
Cl10—Bi1—Cl8	91.92 (11)	Cl6—K1—Cl4	62.42 (9)
Cl11—Bi1—Cl8	90.15 (12)	Cl3^{vi}—K2—Cl10^{v}	160.02 (14)
Cl7—Bi1—Cl8	175.35 (11)	Cl3^{vi}—K2—Cl2	129.64 (14)
Cl12—Bi1—Cl8	128.04 (9)	Cl3^{vi}—K2—Cl1^{iv}	81.68 (13)
Cl10—Bi1—Cl9	120.54 (9)	Cl3^{vi}—K2—Cl12^{v}	109.46 (13)
Cl11—Bi1—Cl9	94.14 (12)	Cl3^{vi}—K2—Cl11^{v}	94.57 (12)
Cl7—Bi1—Cl9	122.82 (9)	Cl12^{v}—K2—Bi1^{v}	40.47 (6)
Cl12—Bi1—Cl9	91.47 (11)	Cl12^{v}—K2—Cl10^{v}	65.44 (9)
Cl8—Bi1—Cl9	86.42 (11)	Cl12^{v}—K2—Cl1^{iv}	143.15 (13)
Cl6—Bi2—Cl4	82.71 (10)	Cl12^{v}—K2—Cl11^{v}	69.13 (9)

Symmetry codes: (i) $x+1, y-1, z+1$; (ii) $x+1, y-1, z$; (iii) $x, y-1, z$; (iv) $x-1, y+1, z$; (v) $x-1, y+1, z-1$; (vi) $x, y+1, z$.

Table S5. Selected bond lengths [Å] and angles [°] for R3PBKC at 353 K.

353 K

Cl6—Bi1—Cl4	100.02 (11)	Cl1—K1—Cl3	64.10 (9)
Cl6—Bi1—Cl5	90.07 (10)	Cl9^{ii}—K1—Cl2	147.30 (14)
Cl5—Bi1—Cl4	88.43 (11)	Cl9^{ii}—K1—Cl3	87.10 (11)
Cl2—Bi1—Cl6	92.61 (10)	Cl6^{v}—K2—Cl4	84.37 (13)
Cl2—Bi1—Cl4	87.88 (10)	Cl6^{v}—K2—Cl10^{iv}	81.87 (11)
Cl2—Bi1—Cl5	175.77 (11)	Cl6^{v}—K2—Cl8^{iv}	145.67 (14)
Cl2—Bi1—Cl3	86.24 (10)	Cl4—K2—Cl8^{iv}	90.67 (14)
Cl1—Bi1—Cl6	85.40 (11)	Cl5^{vi}—K2—Cl6^{v}	135.56 (17)
Cl1—Bi1—Cl4	173.48 (10)	Cl5^{vi}—K2—Cl4	109.39 (15)
Cl1—Bi1—Cl5	95.24 (12)	Cl5^{vi}—K2—Cl10^{iv}	137.88 (14)
Cl1—Bi1—Cl2	88.25 (11)	Cl5^{vi}—K2—Cl8^{iv}	77.98 (11)
Cl1—Bi1—Cl3	89.16 (11)	Cl10^{iv}—K2—Cl4	89.51 (13)
Cl3—Bi1—Cl6	174.47 (11)	Cl10^{iv}—K2—Cl8^{iv}	64.10 (10)
Cl3—Bi1—Cl4	85.35 (11)	Cl11^{iv}—K2—Cl6^{v}	108.39 (15)
Cl3—Bi1—Cl5	91.40 (11)	Cl11^{iv}—K2—Cl4	151.68 (16)
Cl12i—K1—Cl3	139.42 (12)	Cl11^{iv}—K2—Cl5^{vi}	79.57 (12)
Cl2—K1—Cl3	61.03 (8)	Cl11^{iv}—K2—Cl10^{iv}	68.25 (10)

Symmetry codes: (i) x+1, y, z; (ii) x, y+1, z; (iii) x, y, z+1; (iv) x, y, z−1; (v) x−1, y, z; (vi) x, y−1, z.

Table S6. Selected bond lengths [Å] and angles [°] for R3PBKC at 386 K.

386 K			
Cl2—Bi1—Cl4	94.00 (19)	Bi1—Cl2—K1	86.97 (18)
Cl2—Bi1—Cl5	176.6 (2)	Bi1—Cl3—K1	85.3 (2)
Cl2—Bi1—Cl6	89.1 (3)	Bi1—Cl1—K1	91.8 (2)
Cl3—Bi1—Cl2	86.14 (19)	Cl2—K1—Cl3	63.62 (17)
Cl3—Bi1—Cl4	174.9 (2)	Cl2—K1—Cl6^{iii}	80.6 (3)
Cl3—Bi1—Cl5	90.5 (3)	Cl1—K1—Cl5^{ii}	89.7 (3)
Cl3—Bi1—Cl6	89.4 (3)	Cl1—K1—Cl6^{iii}	142.5 (3)
Cl1—Bi1—Cl2	88.20 (19)	Cl4^{i}—K1—Cl2	79.3 (2)
Cl1—Bi1—Cl3	88.2 (2)	Cl4^{i}—K1—Cl3	142.8 (3)
Cl1—Bi1—Cl4	86.7 (2)	Cl4^{i}—K1—Cl6^{iii}	89.1 (3)
Cl1—Bi1—Cl5	91.8 (3)	Cl5^{ii}—K1—Cl2	146.7 (3)
Cl1—Bi1—Cl6	176.6 (3)	Cl5^{ii}—K1—Cl3	85.2 (2)
Cl4—Bi1—Cl6	95.6 (3)	Cl5^{ii}—K1—Cl4^{i}	131.6 (3)
Cl5—Bi1—Cl4	89.4 (3)	Cl5^{ii}—K1—Cl6^{iii}	108.1 (3)
Cl5—Bi1—Cl6	90.8 (4)	Cl6^{iii}—K1—Cl3	82.4 (3)

Symmetry codes: (i) −x+1, y+1/2, −z+1; (ii) −x, y+1/2, −z; (iii) −x, y+1/2, −z+1; (iv) x+1, y, z−1; (v) −x+1, y−1/2, −z+1; (vi) −x, y−1/2, −z; (vii) −x, y−1/2, −z+1; (viii) x−1, y, z+1.

Table S7. Selected bond lengths [Å] and angles [°] for R3PBKC at 413 K.

413 K			
Cl1^{i}—Bi1—Cl1^{iii}	73.5 (10)	Cl1^{iv}—Bi1—Cl1^{v}	73.5 (10)
Cl1^{ii}—Bi1—Cl1^{v}	126.2 (13)	Bi1—Cl1—K1	169.9 (11)

Cl1^{i}—Bi1—Cl1^{iv}	88.2 (7)	Cl1^{viii}—K1—Cl1^{ix}	99.0 (5)
Cl1^{i}—Bi1—Cl1	126.2 (13)	Cl1—K1—Cl1^{viii}	174.6 (11)
Cl1^{iii}—Bi1—Cl1^{ii}	139.2 (14)		

Symmetry codes: (i) x, x−y, −z+1/2; (ii) −x+y+1, y, −z+1/2; (iii) −x+y+1, −x+1, z; (iv) −y+1, −x+1, −z+1/2; (v) −y+1, x−y, z; (vi) −x+y+2, −x+2, z; (vii) −y+2, x−y, z; (viii) x−y+1, −y+2, −z+1; (ix) −x+2, −x+y+1, −z+1; (x) y, x, −z+1; (xi) −x+y+1, −x+2, z; (xii) −y+2, x−y+1, z.